Coalescence of deuterons in relativistic heavy ion collisions

J. L. Nagle and B. S. Kumar
A.W. Wright Nuclear Structure Laboratory, Yale University, New Haven, Connecticut 06520

D. Kusnezov
Physics Department, Yale University, New Haven, Connecticut 06520

H. Sorge and R. Mattiello
Institut für Theoretische Physik, D-60054 Frankfurt am Main 11, Germany
(Received 18 July 1995)

We explore the process of coalescence as a way to create deuterons, antideuterons, and other composite particles in proton+nucleus and nucleus+nucleus collisions. We discuss several approaches to coalescence calculations, and describe in detail some work using an extension to the transport theoretical approach RQMD. We compare our calculations to measured yields of composite particles produced in proton+nucleus and nucleus+nucleus collisions.

PACS number(s): 25.75.Dw, 02.70.Ns, 24.10.Jv

I. INTRODUCTION

The creation of novel states of nuclear and possibly quark matter using relativistic heavy ion collisions has interested many scientists over the past several years [1]. In order to understand the properties of the collision region, it is imperative that experiments be able to give us information on its lifetime and thermodynamic attributes such as temperature, volume, density, and entropy. In particular, a transition of nuclear matter to quark matter is expected to result in a strongly interacting region that lives for a long time, and thus expands to a large volume with large concomitant entropy production.

We discuss below some ways by which one can calculate the abundances of deuterons produced in heavy ion collisions via the mechanism of coalescence. Our initial interest in such calculations was to investigate the dimensions of the collision volume at freeze-out [2]. Our success in describing the yields of deuterons prompted us to investigate how well our techniques applied to studies of the antideuteron [3]. Our work has resulted in an improved understanding of some of the subtleties in doing coalescence calculations. A study of the production of light nuclei should enable us to obtain information that constrains the temperature, baryon density, entropy, and lifetime of the collision volume at ''freeze out.'' We attempt to elucidate some of our ideas in this paper.

We discuss the shortcomings of the simple coalescence and thermal models, and how they can be remedied through use of a coalescence extension to a transport model. We will investigate the effects of source expansion and hydrodynamic flow on the yields of composite particles. We compare the predictions of phenomenological and wave function approaches to coalescence calculations and compare our results with data for light and heavy colliding systems.

II. SIMPLE COALESCENCE MODEL

In 1963, Butler and Pearson developed a model for deuteron formation in proton-nucleus collisions [4]. According to them, ''the proton-neutron pair interacts with the static nuclear optical potential which, together with the usual *p-n* strong force, allows them to bind together to form a deuteron.'' Their calculation used second-order perturbation theory to obtain a relation between the density of deuterons in momentum space and the density of protons and neutrons in momentum space. The key result is that, on account of simple momentum phase space considerations, the deuteron density in momentum space, d^3N_d/dK^3, is proportional to the proton density in momentum space, d^3N_p/dk^3, times the neutron density in momentum space, d^3N_n/dk^3, at equal momentum per nucleon ($K=2k$), and can be expressed as

$$\gamma\frac{d^3N_d}{dK^3}=B_2\left(\gamma\frac{d^3N_p}{dk^3}\right)\left(\gamma\frac{d^3N_n}{dk^3}\right). \tag{1}$$

Since many experiments measure protons but not neuterons, it is useful to rewrite this equation assuming the neutron and proton densities to be identical:

$$\gamma\frac{d^3N_d}{dK^3}=B_2\left(\gamma\frac{d^3N_p}{dk^3}\right)^2, \tag{2}$$

where

$$B_2=|V_0|^2\kappa\left(1+\frac{m^2}{k^2}\right)J(\kappa R). \tag{3}$$

Here m is the nucleon mass, $\kappa^2/m=2.225$ MeV is the binding energy of the deuteron, $|V_0|$ is the depth of the optical potential, and $J(\kappa R)$ is a dimensionless function depending on the optical potential of the target nucleus. Schwarzchild and Zupančic extended this phase space relation to describe the production of various light nuclei in nucleus-nucleus collisions [5]. However, the constant coefficient B_A was no longer thought to represent an admixture of the binding energy of the deuteron and the nuclear optical potential of the target nucleus. For more violent nucleus-nucleus collisions

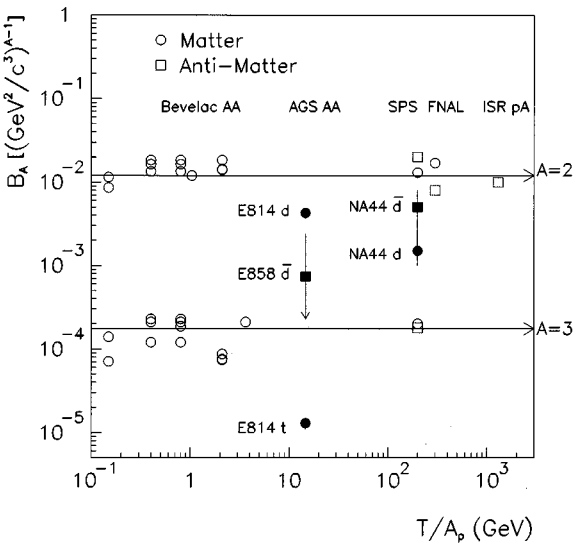

FIG. 1. Coalescence scaling factor B_A for matter and antimatter plotted as a function of the kinetic energy per nucleon T/A (GeV). The data for nuclei are from [6–8,11–13] and the data for the antinuclei are from [7–10,12].

the optical potential for the original nucleus is not a meaningful concept. However, the underlying phase space relationship survives, and is expressed in a form generalized for nuclear species as

$$\gamma \frac{d^3N_A}{dK^3} = B_A \left(\gamma \frac{d^3N_p}{dk^3} \right)^A , \tag{4}$$

where

$$B_A = \left(\frac{2s_A+1}{2^A} \right) \frac{1}{N!} \frac{1}{Z!} (R_{np})^N \left(\frac{4\pi}{3} p_0^3 \right)^{A-1} , \tag{5}$$

s_A is the spin of the cluster of mass A, and N and Z are the neutron and proton numbers of the composite particle. The factor $R_{np}=(N_P+N_T)/(Z_P+Z_T)$, where N_P, Z_P, N_T, and Z_T are the neutron and proton numbers for the projectile and target nuclei. The formulation assumes that the proton and neutron densities are the same except for a scale factor R_{np} which accounts for the initial isospin of the colliding system. The proportionality constant B_A is simply reinterpreted as a function of a momentum radius p_0 within which various pairs of nucleons will fuse. The parameter is phenomenological. However, in this model, it should not change with colliding system and beam energy.

This rather simple picture was used to describe light nuclei production in $A+A$ collisions (systems ranging in mass from C + C to Ar + Pb) at Bevelac energies [6], in higher energy $p+A$ data from the CERN SPS [7], $p+A$ data from Fermilab (FNAL) [8], and $p+p$ data from the CERN ISR [9]. We show as open symbols in Fig. 1 the values B_2 and B_3 measured by many experiments for both matter and antimatter. The data are consistent with the scale factors being independent of energy. It is important to note that the simple phase space relation described in Eq. (4) is applicable to data measured for collisions at a fixed impact parameter, and does not hold if one is dealing with impact-parameter-averaged or minimum bias distributions. However, the experimental data yield relatively constant scale factors for a wide array of colliding systems. This result is surprising and probably indicates that the effects of impact parameter averaging are smaller than the precision with which data and calculations have been compared.

Higher energy (10–15A GeV/c) heavy ion collisions at the BNL-AGS have provided new data for the production of light (anti)clusters. Experiment 858 [10] has measured the scale factor for antideuterons and experiment 814 [11] has measured B_2 for deuterons and B_3 for tritons in Si + Au, Pb collisions at 14.6A GeV/c, as shown in Fig. 1. The scale factors are measured at zero degrees as an average over events at different impact parameters (minimum bias), and both reveal significant deviations from the simple coalescence model. Experiment 814 has also measured the scale factor for deuterons as a function of collision centrality and finds that B_2 decreases by a factor of 40 and B_3 decreases by a factor of 10^4 in going from peripheral collisions to the most central. The discrepancy between the AGS data and the simple models has been attributed to the failure of the model to account for the relative spatial separation of the two nucleons. Preliminary results from experiment NA44 in S + Pb collisions at 200 A GeV/c for B_2 [12] are also shown in Fig. 1. Again significant differences with the simple coalescence model are revealed. It should be noted that the NA44 results are for central (small impact parameter) events and are measured over a range of transverse momenta. Thus caution is warranted when making a comparison between the B_A values obtained in the CERN and AGS measurements. A hint of the discrepancies with the global scaling can also be found in the lower energy Bevalac data for the heaviest projectiles [13,14].

If the size of the colliding system when coalescence is considered is on the order of the size of the deuteron (rms radius = 2.1 fm), then only the relative momentum of the nucleons is a determining factor in their fusion. However, if the system is large enough that two nucleons can be much more than a few femtometers apart, the spatial separations must be considered in calculating the rate of coalescence. Although large A projectiles were used at the LBL Bevalac, few secondary particles are produced due to the low beam energy. Thus, the data are consistent with the collision volume not appearing to expand significantly before freeze-out (though hydrodynamic flow can also affect composite particle yields). The data (except the NA44 result) at higher energies (greater than 200A GeV/c) from SPS, Fermilab, and ISR are for $p+A$ systems. These collisions, therefore, have small interaction volumes despite the significantly higher energy. However, larger $A+A$ systems at AGS and CERN-SPS energies appear to have larger freeze-out volumes.

III. DENSITY MATRIX MODELS

Bond *et al.* [15] developed a fireball model for coalescence using the sudden approximation. In their model, a six-dimensional Wigner density of the composite particle is related to the product of Wigner densities of its ingredients and an overlap of the cluster wave function with the wave functions of its ingredients. Under the assumption that the nucleon phase space distribution is uniform over a volume

TABLE I. B_2 values as functions of rapidity (y) and transverse momentum per nucleon (p_t/A) from experiment 802 for 7% σ_{geom} central Si+Au collisions. The numbers are calculated using measured values for proton and deuteron dN/dy and slopes (T).

y	0.5	0.7	0.9	1.1	1.3	1.5
p_t/A (MeV/c)						
0	1.8×10^{-3}	1.6×10^{-3}	1.6×10^{-3}	1.6×10^{-3}	2.1×10^{-3}	2.6×10^{-3}
200	1.8×10^{-3}	1.7×10^{-3}	1.7×10^{-3}	1.7×10^{-3}	2.2×10^{-3}	2.7×10^{-3}
400	2.0×10^{-3}	2.0×10^{-3}	2.1×10^{-3}	2.0×10^{-3}	2.5×10^{-3}	3.0×10^{-3}
600	2.3×10^{-3}	2.5×10^{-3}	2.7×10^{-3}	2.7×10^{-3}	3.0×10^{-3}	3.5×10^{-3}
800	2.8×10^{-3}	3.5×10^{-3}	3.9×10^{-3}	4.0×10^{-3}	3.8×10^{-3}	4.3×10^{-3}
1000	3.5×10^{-3}	5.0×10^{-3}	5.8×10^{-3}	6.2×10^{-3}	5.0×10^{-3}	5.5×10^{-3}

V, this expression can be cast into a familiar coalescence form as

$$\frac{d^3N_A}{dK^3}=\frac{2s_A+1}{2^A}\left[\frac{(2\pi)^3}{V}\right]^{A-1}(R_{np})^N\left(\frac{d^3N_p}{dk^3}\right)^A, \qquad (6)$$

where $K=kA$ is the momentum of the cluster. As this calculation is nonrelativistic, it does not depend on the relativistic factor γ. A scale factor B_A can still be calculated by comparing the above equation with Eq. (4) (assuming $\gamma\approx1$). This factor will depend inversely on the volume V of the interaction zone.

Sato and Yazaki have used a similar density matrix model [16] to calculate deuteron and triton yields. They assume a sudden approximation when particles cease their interactions. They further assume that the positions and momenta of particles are uncorrelated (namely, no collective expansion). The particle distributions are represented by density matrices and the wave functions of the particles are assumed to be Gaussian in form. Once again, this formalism results in a power law expression for the abundances of nuclei expressed in terms of the abundances of nucleons. In addition, the scale factor B_A can be related to the root mean square radius R_{rms} of the emitting source as

$$B_A=\left(\frac{2s_A+1}{2^A}\right)(R_{np})^N A^{3/2}\left(4\pi\frac{\nu_A\nu}{\nu_A+\nu}\right)^{3/2\,(A-1)}, \qquad (7)$$

where ν_A are the parameters of the Gaussian wave functions and the size parameter ν is related to the rms radius of the excited region as

$$R_{\text{rms}}=\sqrt{\frac{3}{2\nu}}. \qquad (8)$$

The values used for the wave function parameters are $\nu_2=0.20$ fm^{-2} and $\nu_3=0.36$ fm^{-2}.

There are newer calculations that make less restrictive assumptions to include distributed freeze-out times and different source geometries [17]. However, they still do not account for collective expansion, and the position-momentum correlations which we now know exist in the distributions of particles in high energy heavy ion collisions.

IV. THERMODYNAMIC MODEL

A thermodynamic model of heavy ion collisions was developed to describe the production of light nuclei in a rapidly expanding system of nucleons [18]. In the model, quasichemical and thermal equilibrium are maintained since reaction rates are fast compared to nuclear expansion time scales. After a particular stage in the evolution of the collision volume, the model assumes an abrupt transition from a strongly interacting system to a free-streaming one. The nucleon abundances at this time provide information about the volume of the system at freeze-out under the assumption that the phase space density of particles is low, and that quantum statistics can be ignored. The resulting invariant multiplicity of the composite particles can be expressed as

$$\frac{d^3N_A}{dK^3}=\frac{2s_A+1}{2^A}\left[\frac{(2\pi)^3}{V}\right]^{A-1}e^{-E_0/T}(R_{np})^N\left(\frac{d^3N_p}{dk^3}\right)^A. \qquad (9)$$

The parameters of the equation have been defined previously [see Eqs. (4) and (6)]. The exponential factor suppresses excited states with energy E_0 which should be summed over with the appropriate spin factors. Once again, a scale factor can be calculated which will depend inversely on the volume.

V. SPACE-MOMENTUM CORRELATIONS

The above models (barring the simple coalescence model) can explain variations in the scale factor B_A with centrality and colliding system through changes in the source volume. However, they all assume that in the colliding system, the emitted particles have no correlations between their positions and their momenta. Thus, for a given colliding system and centrality, the B_A value should be the same irrespective of the momentum region of the measurement (all momenta sample the entire spatial extent of the source). Much theoretical and experimental work has gone into the description of relativistic heavy ion collisions as exhibiting hydrodynamic flow [19–22]. Such collective expansion will lead to space-momentum correlations. If an experiment measures the scale factor within a limited momentum acceptance, it only samples a portion of the total source spatial distribution. Thus, if the baryon density or the space-momentum correlations vary over the source, one would measure different scale factors at different momenta.

Data from experiment 802 for central collisions of Si + Au at 14.6A GeV/c show that the scale factor B_2 increases with increasing transverse momentum [23]. There also appears to be some rapidity dependence, although one should be cautious in interpreting data at very low rapidities due to

contributions from fragmentation. In Table I we show B_2 values (calculated from measured values of dN/dy and slope) as functions of transverse momentum and rapidity. All of the above analytic models cannot explain the variations in B_2 as a function of the momentum region of the measurement, shown in Table I. Any theory without space-momentum correlations will be unable to reproduce the experimental data.

A rather involved analytic model was formulated by Dover *et al.* [24] and accounts for the longitudinal expansion (some space-momentum correlations) of the source of deuterons. However, in order to obtain analytic solutions, assumptions of boost invariance and simple spatial distributions were still necessary. In addition, no transverse expansion was included and the model would therefore still fail to describe the data of experiment 802.

VI. COALESCENCE EXTENSION FOR TRANSPORT MODELS

Rather than approximate the phase space distribution of particles at freeze-out using an analytic expression, one can use the generated final state of the relativistic quantum molecular dynamics (RQMD) transport model [25] which has been used extensively in describing spectra of produced particles in heavy ion reactions at AGS and CERN-SPS energies. All calculations presented in this paper have been done using RQMD 1.08 [26] in the so-called cascade mode (no potential-type interactions between baryons). Semiclassical transport models such as RQMD do not include the transport of light (anti)clusters and thus such a calculation must be added as an extension.

A. Phenomenological model

The RQMD simulation produces the space-time and momentum-energy four-vectors of all particles at their points of final interaction. Also, the transport model yields a detailed space-time evolution of the system, thereby allowing one to choose when to apply the coalescence calculation. Since the binding energy of the deuteron is quite small (2.225 MeV), the nucleons being considered should not have a high probability of sustaining any collision above this energy (otherwise many of the deuterons calculated would actually be broken up). RQMD tracks all particles down to an interaction energy of 2 MeV, which is a reasonable point at which to do the coalescence calculation.

We first consider a phenomenological parameter model for coalescence. This approach follows the work of Dover *et al.* [27] and Baltz *et al.* [27] who used the cascade code ARC (a relativistic cascade) to predict the abundances of hypernuclei. The procedure we follow considers all possible neutron-proton pairs from each given event. The partner which has its last interaction at an earlier time is propagated to the later time in the two-particle center-of-mass system. In this frame, their relative momentum $\Delta p = |\vec{p_1} - \vec{p_2}|$ and relative spatial separation $\Delta r = |\vec{x_1} - \vec{x_2}|$ are calculated. If they are less than some maximum values ΔP and ΔR, the two nucleons are considered to be a deuteron. These parameters are phenomenological and are determined from matching experimental deuteron data. However, once the parameters are set, they should not vary with colliding system and collision geometry. Additionally, the two nucleons must have the correct spin state $S=1$ to form a deuteron. The spin penalty factor is $\frac{3}{4}$ and is explicitly included as a weight factor multiplying the total deuteron abundances.

In a previous work [2], we found good agreement with deuteron yields from experiments 814 and 802 for Si + Pb, Au interactions at 14.6A GeV/c, using parameters similar to those found by the ARC group (accounting for different definitions since they define their relative momentum as $\Delta p = \frac{1}{2}|\vec{p_1} - \vec{p_2}|$ and relative position as $\Delta r = |\vec{x_1} - \vec{x_2}|$). We found little dependence of the deuteron yield on the exact parameters, assuming the product $(\Delta R \times \Delta P)$ was kept constant. We used this technique to understand the spatial distribution of nucleons as a function of centrality of these collisions.

As we will discuss later, if one looks at deuteron yields in $p+$ Be collisions, one can describe the data in a phenomenological model assuming $\Delta P =$ 300 MeV/c. The value of ΔR can be varied over all values in excess of 2.1 fm without appreciably affecting the predicted abundances of deuterons. This result supports the validity, in collisions of limited spatial extent, of the simple momentum space coalescence approach used before [5].

B. Deuteron production mechanisms

In considering the coalescence of light nuclei, one must be careful to specify the process modeled. At the low energies relevant for big bang nucleosynthesis, the reaction mechanism for deuteron production is primarily $p+n \rightarrow d + \gamma$. Its free space cross sections are used to calculate relative nuclear abundances. However, the free space $p+n$ capture cross section is too small (only 0.1 mb at 10 MeV/c relative momentum) to account for the yields of deuterons in relativistic heavy ion collisions (where the conditions are significantly different from the relatively long-lived low density universe). Another possible deuteron-forming reaction is $N+N \rightarrow d+\pi$. The additional particle, here the pion, is required in order to conserve momentum and energy in a reaction with two ingoing nucleons. In principle, there are more complicated processes which can produce a deuteron in an NN collision. However, their rates are expected to be rather small because cluster formation is not favorable from phase space arguments.

There is another class of processes which allow for deuteron formation in the final state: three-nucleon collisions, more generally 3,4, . . . -body collisions, with a nucleon pair in the ingoing state. The cross sections for such processes are significantly higher, but now require at least three particles to be in close proximity (with two of them being nucleons close in momentum space). Recently, Danielewicz and Bertsch have developed a model for deuteron production [28] employing the impulse approximation. They multiply their result with an energy-dependent factor in order to account for deviations from experimental data which were measured in reactions going in the reverse direction ($p+d \rightarrow p+p+n$). The strengths of these transitions in the two directions are related by detailed balance. As a by-product of this approach, the dynamics of deuteron propagation can be studied in a transport theoretical framework. The deuterons are treated as

just another species in addition to the nucleons, pions and other particles [28]. In principle, such an approach is best suited to calculate deuteron yields in simulations of nucleus-nucleus collisions. However, the crucial ingredient is a good knowledge of the transition rates (for example, $p+d\rightarrow p+p+n$). The reaction strength has to be known as a function of all independent relativistic invariants which can be formed from the three-momenta on the right-hand side of this type of reaction. Such detailed knowledge does not exist presently.

C. Wigner function approach

Nuclear cluster formation is a truly quantum-mechanical (bound state) problem beyond the limits of applicability for semiclassical transport theory. However, one can give approximate solutions for ''weakly'' bound systems employing the formalism of Wigner transforms [29–31]. A ''weakly bound state'' means that the binding energy is small compared to all relevant mass scales, particle masses, and typical kinetic energies in the problem. Here it is assumed that since the deuteron binding energy is very small, one can treat the problem as if the deuteron were a state near threshold, but in the continuum. It is tacitly assumed that other particles in the neighborhood of the np pair absorb the excess energy due to bound-state formation *without* changing the transition probabilities.[1] If one knows the proton-neutron (two-body) density matrix $\hat{\rho}_{pn}(t)$ of a system at a given time,[2] one can calculate the number of deuterons with given momentum $\vec{P_D}$ as

$$\frac{d^3N_D}{dP_D^3}=\mathrm{Tr}[\hat{\rho}_D\hat{\rho}_{pn}(t)]. \tag{10}$$

$\hat{\rho}_D=|\Psi_D\rangle\langle\Psi_D|$ is the projector onto the np pair in the deuteron state and Ψ_D is the bound-state wave function for a deuteron with some given momentum. The final number of deuterons is given by taking the limit $t\rightarrow\infty$.

In order to solve the problem, the pn two-particle phase space density from the transport model must be related to the pn two-particle density operator. One can make the connection using the Wigner representation of the density operator. The Wigner transformation is just a particular representation of quantum mechanics. Every single-particle operator $\hat{A}$ is represented by a function in phase space [32],

$$A^{\mathrm{Wigner}}(p,x)=\int dy e^{-ipy}\langle x+\tfrac{1}{2}y|\hat{A}|x-\tfrac{1}{2}y\rangle, \tag{11}$$

with a straightforward generalization to $2,\ldots,N$-particle operators. The N-body density operator can be transformed to the Wigner representation (referred to as the Wigner density)

$$\rho_N^{\mathrm{Wigner}}(p_1,x_1,p_2,x_2,\ldots,p_N,x_N)=\int dy_1\cdots dy_N e^{-ip_1y_1}\cdots e^{-ip_Ny_N}\langle x_1+\tfrac{1}{2}y_1,\ldots,x_N+\tfrac{1}{2}y_N|\hat{\rho}_N|x_1-\tfrac{1}{2}y_1,\ldots,x_N-\tfrac{1}{2}y_N\rangle. \tag{12}$$

The pn two-particle Wigner density can be simply obtained either by integrating the N-particle Wigner density over all coordinates except for a proton and a neutron or by Wigner transforming the pn two-body density matrix $\hat{\rho}_{pn}(t)$. The Wigner density, when integrated over the momenta, yields the probability distribution in the coordinate representation and also, when integrated over space, yields the probability distribution in momentum space. The overall normalization is defined to be h^3 for integration over both coordinate and momentum space. One must keep in mind that while the Wigner density appears formally as a probability density, it is only a quasiprobability, in that its sign can be positive or negative at a given point in phase space, while its integral over any unit phase space cell is positive semidefinite.

Equation (13) provides the ''bridge'' between semiclassical transport theory by identifying the semi-classically generated N-body phase space distribution from the transport calculation with the N-body Wigner density as

$$\rho_{pn}^{\mathrm{Wigner}}\approx\left\langle\sum_{(pn)}\prod_{i=p,n}h^3\delta^3(\vec{x_i}-\vec{\tilde{x}}_i(t))\delta^3(\vec{p_i}-\vec{\tilde{p}}_i(t))\right\rangle, \tag{13}$$

where $\vec{\tilde{x}}_i$ and $\vec{\tilde{p}}_i$ are the positions and momenta given by the transport calculation. The angular brackets denote averaging over all collisions at the same impact parameter. In addition, the two-particle operator projecting onto the deuteron wave state with momentum $\vec{P_D}=(\vec{p_n}+\vec{p_p})$ can be written in the Wigner representation as

[1] We expect this approximation to work much better in ultrarelativistic AA collisions than in the environment of nuclear collisions at a few hundred MeV's where this model was studied first. In the region of multifragmentation, the typical excitation energies at freeze-out are around 5 MeV, giving an average kinetic energy per nucleon not very large on the scale of the deuteron binding energy. In contrast, the characteristic freeze-out temperature at high energy at the AGS is expected to be on the order of 100–150 MeV.

[2] This is strictly true only in the nonrelativistic approximation which is appropriate if one considers the problem in a frame in which the deuteron momentum is small.

$$\rho_D^{\text{Wigner}}(\vec{P}_D;\vec{r},\vec{q}=\delta^3(\vec{P}_D-(\vec{p}_n+\vec{p}_p))\int d\vec{y}e^{-i\vec{q}\cdot\vec{y}}\Psi_D\left(\vec{r}+\frac{\vec{y}}{2}\right)\Psi_D^*\left(\vec{r}-\frac{\vec{y}}{2}\right), \tag{14}$$

where Ψ_D is the deuteron wave function and $\vec{q}=\frac{1}{2}(\vec{p_1}-\vec{p_2})$ and $\vec{r}=(\vec{r_1}-\vec{r_2})$.

The trace in Eq. (10) can be rewritten as a phase space integral giving the momentum density of deuterons

$$\frac{d^3N_D}{dP_D^3}=\int dx_p dp_p dx_n dp_n(\rho_D^{\text{Wigner}}\rho_{pn}^{\text{Wigner}}). \tag{15}$$

This expression may appear ''classical,'' but is valid quantum mechanically with the density operators written in the Wigner representation [31]. Thus, using Eqs. (13)–(15) allows one to determine at arbitrary times the ''deuteron content'' of the state which is generated in a semiclassical transport calculation. Each interaction in the transport calculation which involves a nucleon will change the deuteron content. This can be written as the change in probability of a nucleon pair to be in a deuteron state, ''before'' and ''after'' each collision with another third hadron (see [30]).

Of course, by taking the phase space density from the transport calculation, the deuteron content would also change (decrease steadily) after the stochastic interactions have ceased. The particles are streaming freely on classical trajectories and are not subject to forces which may lead to deuteron states. If, however, the nucleon pairs were propagated quantum mechanically, with a Hamiltonian whose energy spectrum contains the deuteron state, the formation probability would remain constant [30]. As a consequence, the final deuteron content based on the semiclassical dynamics is ''realistically'' calculated only just after the last interactions in the model have ceased and before free streaming sets in. Of course, the degree of correctness depends on how well the dynamics of the collision before freeze-out is incorporated in the transport model.

Thus, the final deuteron yields are calculated from the proton-neutron-pair phase space distribution $\rho_{pn}^{\text{Wigner}}$ at freeze-out with the Wigner transform of the deuteron wave function as a weighting factor, integrated over phase space and freeze-out time:

$$\frac{d^3N_D}{dP_D^3}=\int d^4x_1 d^4x_2\int d^3p_1 d^3p_2\rho_{pn}^{\text{Wigner}}(p,\vec{x}_1,\vec{p}_1;n,\vec{x}_2,\vec{p}_2)p_d(1,2). \tag{16}$$

The ''coalescence factor'' p_d is calculated as

$$p_d=\tfrac{3}{8}\,\delta^3(\vec{P}_D-(\vec{p}_n+\vec{p}_p))\rho_D^{\text{Wigner}}(\vec{r}_{\text{c.m.s.}},\vec{q}_{\text{c.m.s.}}). \tag{17}$$

ρ_D^{Wigner} denotes the Wigner transform of the deuteron wave function, with center-of-mass motion removed. Its arguments are the distance between the nucleons at the larger of the two freeze-out times and the relative momentum, all values evaluated in the deuteron center of mass frame where $\vec{p}_1+\vec{p}_2=\vec{0}$. While ρ_D^{Wigner} gives the probability density for an np pair to form a deuteron given their spatial and momentum coordinates, the factor 3/8 comes from the projection of the assumed uncorrelated spin-isospin quantum numbers of the n and the p onto the corresponding deuteron quantum numbers $(I=0,S=1)$. Calculations using this method at AGS energies are described in the literature [3,33].

We are aware that a subset of deuterons result from neutron-proton pairs with freeze-out coordinates defined by collisions between the very nucleons in the pair. Ideally, such a collision should be discarded and the interactions with other hadrons should define the freeze-out coordinates. However, we have circumvented this problem and find, by comparing to results based on the event-mixing technique (independent particle approximation) for nucleus-nucleus collisions, that the deuteron yields without event mixing are higher by (15–25)%.

The prefactor from spin-isospin projection differs from the factor used in [27,30,34,35] by 1/2, because those calculations have not accounted for an isospin projection. No penalty factor for isospin is included in the phenomenological parameter coalescence method [27]. However, since the cutoff parameters ΔR and ΔP are phenomenological, such a factor can simply be ''absorbed,'' which is no longer the case in the wave function approach. In using the intranuclear cascade (INC) code to simulate collisions at Bevelac energies [30], the authors found good agreement with data within theoretical and experimental uncertainties of order 50%. This implies that a factor of 2 caused by statistical isospin projection instead of the assumed isospin matching is in the range of the estimated error bars.

Note that quantum statistics (antisymmetrization of the many-nucleon wave function) does not generate such an isospin suppression factor. Projecting in the internal quantum number space on $I=0$ and $S=1$ forces the spatial part of the wave function to be symmetric under particle exchange. Antisymmetrization under particle exchange is always reflected on the Wigner function level by the requirement that the many-particle Wigner function in phase space be symmetric under particle exchange, a property which is fulfilled by the semiclassically generated phase space distribution. It has been suggested that one could order the projections by first performing the spin projection and then the projection on the

s-wave state for the relative motion of the two nucleons [36]. After these projections the isospin part of the two-nucleon Wigner function would be nonzero only in the antisymmetric ($I=0$) isospin part. However, the knowledge about the two-nucleon state at freeze-out in momentum space changes accordingly after these projections. For instance, if the two-nucleon system would be specified by a superposition of plane waves initially, only the $P_{l=0}$ parts would survive the projection and would therefore change the Wigner function of the two-particle state in phase space as well. Such a calculation has not been done yet.

An important point of relevance here is that RQMD neglects the influence of the force leading to deuteron formation during the dynamical evolution of the collision. Its Hamiltonian disregards the presence, location, and possible disappearance of the deuteron state in the medium. Hence one is obliged to assume uncorrelated spin and isospin quantum numbers for the n and the p, and use a $\frac{3}{4}\times\frac{1}{2}$ weight factor when calculating deuteron yields. The isospin factor cannot be ignored since the d is an eigenstate of the total isospin of the two particles, and the n and the p individually are not. It may be instructive to study the dependence of the final d yield on the ordering of the spin and orbital angular momentum projections which could reveal some of the intrinsic limitations of this semiclassical approach. Of course, we would not expect any influence from changing the ordering of the projection operators on the deuteron state if the calculations were done with the exact Hamiltonian at all times.

D. Choice of deuteron wave function

One must choose the form of the wave function of the two nucleons in the deuteron state to construct a deuteron Wigner density ρ_D^{Wigner}. The simplest such wave function is from the square well potential which roughly motivates our choice of phenomenologicial parameters [2]. The next choice would be the harmonic oscillator wave function which has the advantage that the Wigner density can be solved analytically. Following Eq. (14), one finds the Wigner density for the deuteron (with the center-of-mass motion removed) as

$$\rho_D^{\text{Wigner}}(\vec{r},\vec{q}) = 8e^{-r^2/d^2 - q^2d^2}, \tag{18}$$

where $d=1.7$ fm (to match the rms radius of the deuteron, 2.1 fm).

We have also calculated the Wigner density from the Hulthen wave function solution to the Yukawa potential [37]. This choice of potential has the disadvantage of a Wigner density which cannot be solved analytically. We have approximated the Hulthen wave function with a parametrization (a basis set of 15 central symmetric Gaussians) which can then be Wigner transformed analytically [33]. This approximation of the Wigner density is able to match the normalization condition to better than 0.5%.

We can make a direct comparison of the deuteron Wigner densities from the two wave functions. The harmonic oscillator Wigner density yields rms values of $|\vec{r}| = 2.02$ fm and $|\vec{q}| = 144$ MeV/c, and the Hulthen wave function Wigner density yields $|\vec{r}| = 2.92$ fm and $|\vec{q}| = 109$ MeV/c. These values are similar and thus our calculations using these densities should have relatively similar predictions. Plotted in Fig. 2 are contour lines of the Wigner density shown as functions of $|\vec{r}|$ and $|\vec{q}|$ for the harmonic oscillator and Hulthen wave functions. The Hulthen Wigner density is shown here for $\theta=\pi/2$ (θ is the angle between the relative position and relative momentum vectors). It should be noted that the Wigner density is maximal at this angle. The Wigner density for the harmonic oscillator is independent of θ as shown in Eq. (18). The values are relatively similar, although the contour lines curve in opposite directions. This curvature gives a greater deuteron yield for the Hulthen case from nucleons with very small relative momentum and quite large relative positions. It should be emphasized at this point that this entire approach is semiclassical. In a true quantum-mechanical picture, one could not discern details within regions of phase space limited by the uncertainty principle. Thus, although one can see detailed differences between the models in the Wigner density, perhaps the overall density should be averaged over regions of order $\hbar^3$.

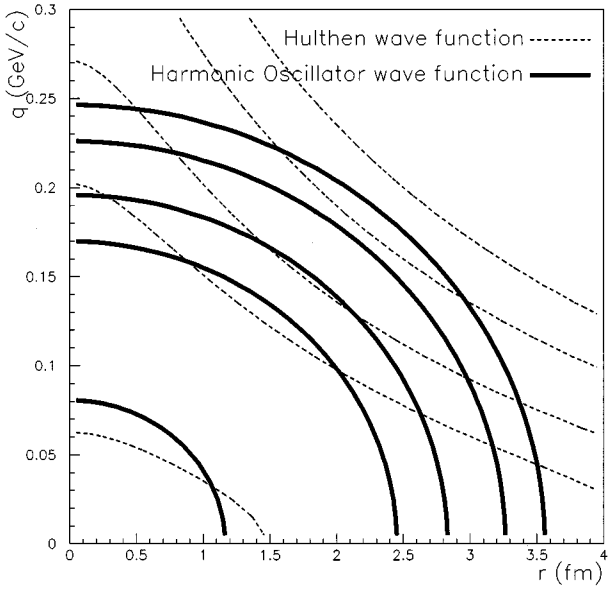

FIG. 2. Wigner density contour map as functions of relative space ($r=|(\vec{r_1}-\vec{r_2}|$) and momentum ($q=|\frac{1}{2}(\vec{p_1}-\vec{p_2})|$) for harmonic oscillator and Hulthen wave functions (with $\theta=\pi/2$). Contour lines are at Wigner density values of 5.0, 1.0, 0.5, 0.2, and 0.1.

The value of $d=1.7$ fm in the harmonic oscillator model corresponds to a rms radius of 2.1 fm for the deuteron. However, Gyulassy *et al.* [30] vary the value of d by factors of 2 and find little sensitivity to the scale chosen, which implies that the nucleon phase space distributions do not change appreciably over the spatial and momentum range of the deuteron. Thus, the calculations are not sensitive to the choice of the exact deuteron wave function. We have attempted similar calculations and find little sensitivity to the parameter d, except in very small colliding systems like p + Be where finite size effects are important. Similarly, by comparing the

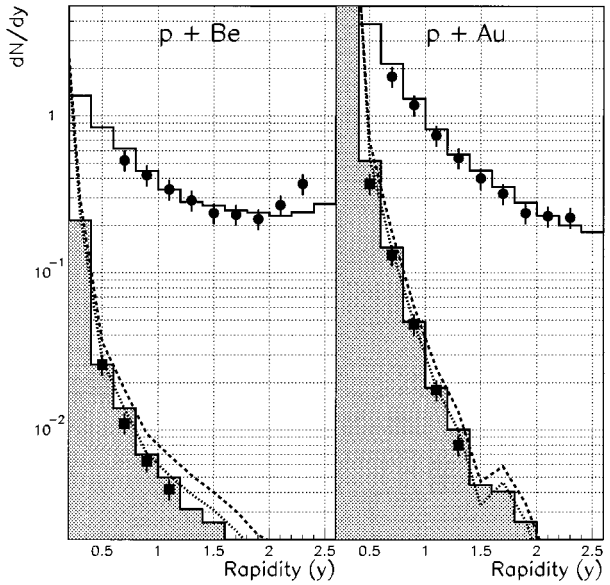

FIG. 3. dN/dy for protons (circles) and deuterons (squares) from p + Be and p + Au minimum bias collisions from experiment 802 [40]. The shaded histograms are the parameter model prediction for deuterons. The harmonic oscillator and Hulthen wave function results are shown as dotted and dashed curves, respectively.

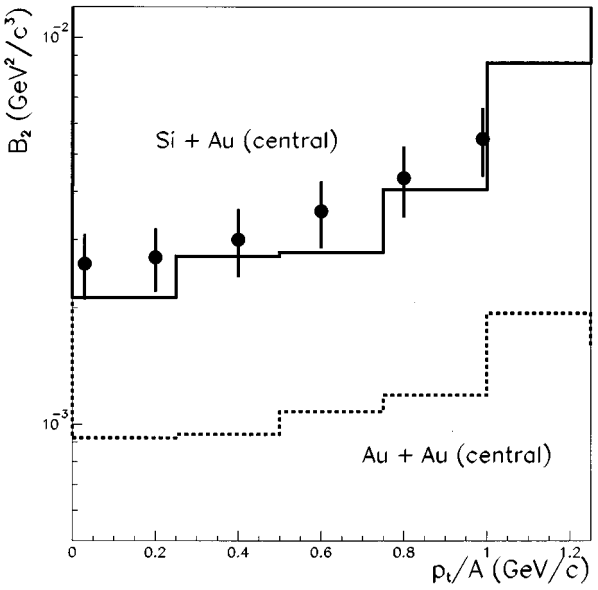

FIG. 5. RQMD B_2 values (with a rapidity window of one unit around midrapidity) are shown as a function of the transverse momentum per nucleon for Si + Au central ($b=2$ fm) and Au + Au central ($b=3$ fm) collisions. RQMD deuterons are calculated using the harmonic oscillator wave function. Extrapolated data points from experiment 802 for Si + Au collisions (Table I) are shown.

harmonic oscillator and Hulthen wave functions one can gauge the sensitivity of the results on the exact form of the wave function used.

VII. COMPARISONS WITH DATA

In studies of the production of nuclei, it is important to make a distinction between the processes of coalescence and fragmentation. Fragmentation of the projectile and target nuclei results in the production of light nuclei whose rapidities should nominally be similar to those of the projectile and target. The widths of the fragmentation peaks can be determined from a knowledge of the Fermi momenta p_F of the nucleons in the interacting nuclei, which are known to be $\approx$ 270 MeV/c nearly independent of A (except for the lightest nuclei with lower densities). This momentum would spread the fragmentation peak by $\Delta y \approx 0.33$ around target rapidity ($y=0$). If light nuclei are detected in the midrapidity region beyond these Fermi momentum limits, they would have undergone a large shift in momentum. Given the low

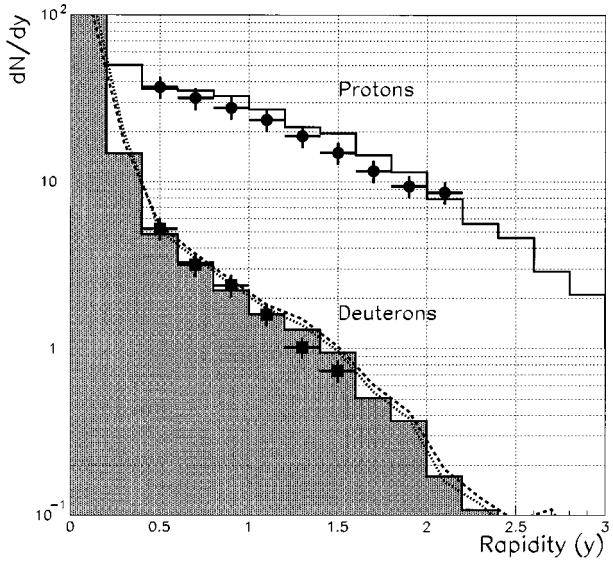

FIG. 4. dN/dy for protons and deuterons from Si + Au central collisions from experiment 802 [23] and predictions of RQMD.

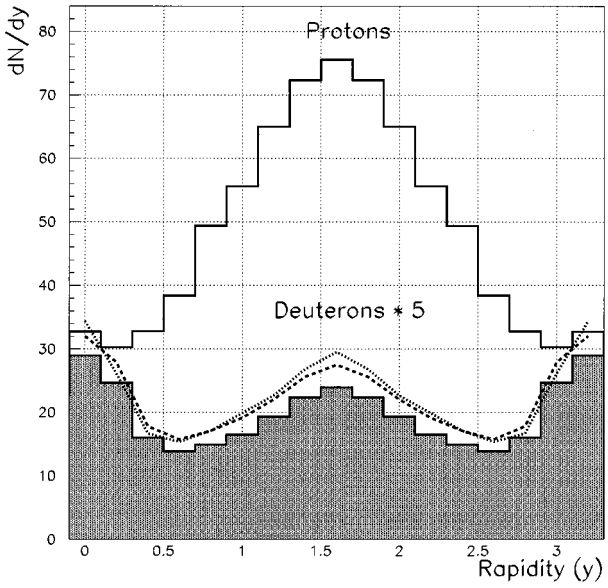

FIG. 6. dN/dy for protons and deuterons calculated for Au + Au ($b=3$ fm) interactions using RQMD.

binding energy of the deuteron, this momentum shift would have to occur via numerous small momentum kicks. Single collisions resulting in large momentum shifts would break up the light nuclei into their constituents. Thus, nuclei in the midrapidity region are not fragments but can only be formed through the coalescence of nucleons after all interactions have ceased. In order to stay away from fragmentation regions, in our previous work to estimate source sizes [2], only deuterons at least 1.1 units in rapidity away from target or beam rapidity were used.

In all these calculations, higher mass nuclei ($A>2$) are assumed to have a negligible effect on the deuteron spectra. This assumption is not always good in the fragmentation region, but in the midrapidity region of coalescence the number of light nuclei heavier than the deuteron is significantly suppressed. Recent results of experiment 878 in Au + Au collisions at 10.8A GeV/c find that the ratio $t(^3\mathrm{He})/d \approx {}^4\mathrm{He}/t(^3\mathrm{He}) \approx 1/50$ at $p_t = 0$ and midrapidity $y = 1.6$ [38].

One of the major goals of light nuclei studies is the determination of the source volume. If we model the coalescence process correctly, we still only expect to match the experimental data if the transport model matches the total collectivity and system expansion before particles cease interacting. In the following, we compare the results of our calculations with data for light as well as heavy systems to test the model predictions in simple as well as complex environments.

The simplest colliding system studied at AGS energies [(10–15)A GeV/c] is p + Be at 14.6 GeV/c. With only one projectile nucleon and a small target, the total number of secondary collisions and complex resonance excitations is severely limited. Thus, if RQMD can match the distributions of elementary particles like protons and pions, we might assume that the model has the correct description of the collision dynamics.

As shown in Fig. 3, RQMD (version 1.08) matches the proton dN/dy data of experiment 802 for minimum bias collisions [40]. First, we use the phenomenological parameter coalescence model to calculate the deuteron yields. These are shown as the shaded histogram. We find reasonable agreement with experimental data when the values of $\Delta R = 2.3$ fm and $\Delta P = 0.300$ GeV/c are used. Applying the wave function method, we find that the harmonic oscillator and Hulthen wave function predictions agree with each other and with the data to within 30% as shown by curves in the same figure. All the predictions are in reasonable agreement with experimental data which have (10–15)% systematic errors in addition to statistical errors. Shown in the same figure are similar data and models for p + Au collisions at 14.6 GeV/c. The agreement between the model and the data is reasonable.

Applying the same techniques to Si + Au collisions at 14.6 A GeV/c, we compare in Fig. 4 the calculations with dN/dy data from experiment 802. We find good agreement between the various predictions of RQMD and the data at the level of 30%. The phenomenological parameters seem to give lower yields by (10–20)% compared to the wave function methods for all systems. It is not immediately obvious whether this is in better agreement with experimental data since systematic uncertainties in the data are at the level of (10–15)%.

In Fig. 5 we show, using proton and deuteron spectra from RQMD, calculated values of B_2 for Si + Au (impact parameter $b=2$ fm) events plotted as a function of p_t/A. The values are calculated in a rapidity region of width one unit around midrapidity. The B_2 values from experiment 802 at rapidity $y=1.5$ from Table I are also plotted and show reasonable agreement with RQMD. It should be noted that the rapidity ranges are not exactly matched; however, the B_2 values do not depend strongly on rapidity over this region.

In a previous publication [2], we found good agreement using parameters $\Delta R = 3.8$ fm and $\Delta P = 0.185$ GeV/c with deuteron data for Si + Au, Pb data of experiments 814 and 802. We found that one could reproduce the data while varying the parameters and keeping the product of the two constant ($\Delta R \times \Delta P \approx 700$ MeV fm). For this lighter p + Be system, the above parameters underpredict the deuteron yield because of finite size effects ($\Delta R = 3.8$ fm is larger than the system size at freeze-out). The new parameters with smaller ΔR and larger ΔP values now represent a set of parameters that are able to reproduce the data from $p+A$ and Si + A collisions at the AGS energies.

Data from Au + Au collisions at 11A GeV/c for deuterons should be available soon from experiments 864, 878, 886, and 877. Applying the coalescence methods described and using Au + Au events generated with RQMD, we can predict deuteron spectra. In Fig. 6, we show dN/dy spectra for protons and deuterons for central events (impact parameter $b=3$ fm). Again we see reasonable agreement among the coalescence predictions, with the wave function methods overpredicting the cutoff parameter yield by a small margin. In Fig. 5 we show, using proton and deuteron spectra from RQMD, calculated values of B_2 for Au + Au ($b=3$ fm) events plotted as a function of p_t/A. One sees that again B_2 varies with phase space. In effect, this plot is a map of the correlated baryon density for particles within a given momentum region.

In RQMD compression-induced effects can be included, because this transport model contains optional potential-type interactions between baryons [39]. The collective (hydrodynamic-type) behavior of compressed matter increases under the influence of these repulsive mean fields [33]. The influence of various types of potentials or mean fields on the nuclear reaction dynamics at ultrarelativistic energies deserves further study. Nuclear clusters are a particularly useful probe, because heavy particles exhibit collective flow much better than hadrons with light masses. Work in this direction is in progress. Comparisons of such predictions with experimental data should be extremely useful in understanding hydrodynamic flow in heavy ion collisions.

VIII. CONCLUSIONS

The Wigner density approach shows good agreement with the experimental deuteron data for a large number of colliding systems and centralities. Also, a common set of phenomenlogical parameters ΔR and ΔP reproduces the experimental data. The predictions are not sensitive at the level of 30%

to the coalescence method used. This result is promising. Further studies of cluster formation are certainly warranted to gain insight into the nucleon source size and collective flow. The effects of an expanding collision volume and hydrodynamic flow should increase for larger colliding systems (Au + Au at the AGS and Pb + Pb at CERN) and should provide exciting new physics.

ACKNOWLEDGMENTS

We are pleased to acknowledge useful and stimulating discussions with R. Shankar, S. Mrowczynski, J. Sandweiss, P. Stankus, and C. Dover. This work was supported in part by Grant No. DE-FG02-91ER-40609 with the U.S. Department of Energy.

[1] For example, see articles in *Quark Matter '95*, Proceedings, edited by A. Poskanzer, J. W. Harris, and L. S. Schroeder [Nucl. Phys. **A590**, Nos. 1, 2 (1995)].
[2] J.L. Nagle *et al.*, Phys. Rev. Lett. **73**, 1219 (1994).
[3] J.L. Nagle *et al.*, Phys. Rev. Lett. **73**, 2417 (1994).
[4] S.T. Butler and C.A. Pearson, Phys. Rev. Lett. **7**, 69 (1961); Phys. Rev **129**, 836 (1963).
[5] A. Schwarzschild and C. Zupančic, Phys. Rev. **129**, 854 (1963).
[6] S. Nagamiya *et al.*, Phys. Rev. C **24**, 971 (1981); R.L. Auble, *ibid.* **28**, 1559 (1983); M. Anikina, JINR Report No. 1-84-216, Dubna, 1984.
[7] W. Bozzoli, Nucl. Phys. **B144**, 317 (1978).
[8] J.W. Cronin *et al.*, Phys. Rev. D **11**, 3105 (1975).
[9] W.M. Gibson *et al.*, Lett. Nuovo Cimento **21**, 189 (1978); K. Guettler *et al.*, Nucl. Phys. **B116**, 77 (1976); J.C.M. Armitage *et al.*, *ibid.* **150**, 87 (1979).
[10] E858 Collaboration, A. Aoki *et al.*, Phys. Rev. Lett. **69**, 2345 (1992).
[11] E814 Collaboration, J. Barrette *et al.*, Phys. Rev. C **50**, 1077 (1994).
[12] J. Simon-Gillo *et al.*, in [1].
[13] M.C. Lemaire *et al.*, Phys. Lett. **85B**, 38 (1979).
[14] S. Wang *et al.*, Phys. Rev. Lett. **74**, 2646 (1995).
[15] R. Bond, P.J. Johansen, S.E. Koonin, and S. Garpman, Phys. Lett. **71B** 43 (1977).
[16] H. Sato and K. Yazaki, Phys. Lett. **98B**, 153 (1981).
[17] S. Mrowczyinski, Phys. Lett. B **277**, 43 (1992); P. Danielewicz and P. Schuck, *ibid.* B **274**, 268 (1994); V.L. Lyuboshits, Sov. J. Nucl. Phys. **48**, 956 (1988).
[18] A.Z. Mekjian, Phys. Rev. Lett. **38**, 604 (1977); Phys. Rev. C **17**, 1051 (1978); S. Das Gupta and A.Z. Mekjian, Phys. Rep. **72**, 131 (1981).
[19] H. Stöcker *et al.*, in [1].
[20] P. Braun-Munzinger, J. Stachel, J.P. Wessels, and N. Xu, Phys. Lett. B **344**, 43 (1995).
[21] E. Schnedermann and U. Heinz, Phys. Rev. Lett. **69**, 2908 (1992); Phys. Rev. C **47**, 1738 (1993).
[22] E877 Collaboration, J. Barrette *et al.*, Phys. Rev. Lett. **73**, 2532 (1994).
[23] E802 Collaboration, T. Abbott *et al.*, Phys. Rev. C **50**, 1024 (1994).
[24] C.B. Dover, U. Heinz, E. Schnedermann, and J. Zimanyi, Phys. Rev. C **44** 1636 (1991).
[25] H. Sorge, H. Stöcker, and W. Greiner, Ann. Phys. (N.Y.) **192**, 266 (1989).
[26] H. Sorge, L. Winckelmann, H. Stöcker, and W. Greiner, Z. Phys. C **59**, 85 (1993).
[27] C. Dover *et al.*, in HIPAGS '93 [Report No. MITLNS-2158, 1993], p. 213; A.B. Baltz *et al.*, Phys. Lett. B **325**, 7 (1994).
[28] P. Danielewicz and G. Bertsch, Nucl. Phys. **A533**, 712 (1991).
[29] E.A. Remler, Ann. of Phys. (N.Y.) **136**, 293 (1981).
[30] M. Gyulassy, K. Frankel, and E.A. Remler, Nucl. Phys. **A402**, 596 (1983).
[31] G.F. Bertsch, Nucl. Phys. **A400**, 221c (1983).
[32] R.P. Feynman, *Statistical Mechanics* (Benjamin, Reading, MA, 1972).
[33] R. Mattiello *et al.*, Phys. Rev. Lett. **74**, 2180 (1995).
[34] L. Csernai and J. Kapusta, Phys. Rep. **131**, 854 (1986).
[35] Z. Arvay, J. Zimanyi, T. Csorgo, C.B. Dover, and U. Heinz, Z. Phys. A **348**, 201 (1994). This paper uses an isospin factor in the quark basis, and not in the hadronic basis.
[36] C. Dover (private communication).
[37] R.G. Sachs, *Nuclear Theory* (Addison-Wesley, Cambridge, MA, 1955).
[38] E878 Collaboration, D. Beavis *et al.*, Phys. Rev. Lett. **75**, 3078 (1995).
[39] H. Sorge, R. Mattiello, H. Stöcker, and W. Greiner, Phys. Rev. Lett. **68**, 286 (1992); and H. Sorge, H.v. Kleitz, R. Mattiello, H. Stöcker, and W. Greiner, Z. Phys. C **47**, 629 (1990).
[40] E802 Collaboration, T. Abbott *et al.*, Phys. Rev. D **45**, 3906 (1992)